

Middle Pliocene sea surface temperature variability

Harry J. Dowsett,¹ Mark A. Chandler,² Thomas M. Cronin,¹ and Gary S. Dwyer³

Received 11 January 2005; revised 25 March 2005; accepted 8 April 2005; published 10 June 2005.

[1] Estimates of sea surface temperature (SST) based upon foraminifer, diatom, and ostracod assemblages from ocean cores reveal a warm phase of the Pliocene between about 3.3 and 3.0 Ma. Pollen records and plant megafossils, although not as well dated, show evidence for a warmer climate at about the same time. Increased greenhouse forcing and altered ocean heat transport are the leading candidates for the underlying cause of Pliocene global warmth. Despite being a period of global warmth, this interval encompasses considerable variability. Two new SST reconstructions are presented that are designed to provide a climatological error bar for warm peak phases of the Pliocene and to document the spatial distribution and magnitude of SST variability within the mid-Pliocene warm period. These data suggest long-term stability of low-latitude SST and document greater variability in regions of maximum warming.

Citation: Dowsett, H. J., M. A. Chandler, T. M. Cronin, and G. S. Dwyer (2005), Middle Pliocene sea surface temperature variability, *Paleoceanography*, 20, PA2014, doi:10.1029/2005PA001133.

1. Introduction

[2] During the Pliocene epoch (5.2–1.8 Ma) the Earth climate system shifted from a period of high-frequency–low-amplitude variability to one of high-frequency–high-amplitude variability characteristic of the Pleistocene glacial-interglacial cycles. Stable isotopic and faunal data from marine cores show marked changes in biogeography during the early and mid-Pliocene relative to today. Evidence from those same cores supports major changes in global ice volume and concomitant sea level changes. Individual time series indicate a strong obliquity-driven component to the climate system [Dowsett *et al.*, 1999].

[3] In a synoptic sense, the sea surface temperature reconstructions of the mid-Pliocene do not appear especially different from the present climate. On closer inspection, however, it is apparent that while patterns of warming and cooling are similar, their magnitudes are not. Gulf Stream warmth in the North Atlantic extended farther north into the true Arctic, relative to today. Likewise, important oceanic fronts in the Southern Ocean were situated significantly closer to the Antarctic continent during the mid-Pliocene. Seasonality was also decreased relative to today in many regions, resulting in the “warm equable climate” ascribed to the Pliocene by so many previous workers [Zubakov and Borzenkova, 1988, 1990].

[4] The U.S. Geological Survey’s Pliocene Research, Interpretation, and Synoptic Mapping (PRISM) reconstruction [Dowsett *et al.*, 1994, 1996, 1999] is based upon time series which each have their own variability. Chronostrati-

graphic methods are not precise enough to make accurate point-to-point correlations between all localities on the suborbital scale. Rather than using an exact time slice approach, PRISM uses a “time slab,” which represents about 300 kyr of Earth history (Figure 1). The rationale is that all localities can be confidently correlated to the interval represented by the slab, but not necessarily to each other. While the amplitude of obliquity forcing is relatively constant throughout the PRISM interval (lower amplitude than the time prior to or immediately after), precessional cycles have higher amplitude in the later part of the band than in the 3.3 to 3.2 Ma interval (Figure 1). Because of the variability observed within the 300 kyr time slab, the PRISM reconstruction utilizes a peak averaging methodology [Dowsett and Poore, 1991]. The implication is that the climate represented by the PRISM reconstruction is an average state. There are data from all localities that point toward both higher and lower degrees of warming in the original PRISM data [Dowsett *et al.*, 1999]. Since one of the initial goals of the PRISM Project was to provide a digital data set useful for modeling experiments, it has become necessary to capture some of the variability in the original data and develop additional data sets that “bracket” the mid-Pliocene warming.

[5] The primary goal of this work then is to develop maximum and minimum possible warming data sets (PRISM-MAX, PRISM-MIN [see Dowsett, 2004]), which can be used, along with the present PRISM2 reconstruction, for modeling experiments. The result is a climatological error bar for the warm peak phases of the mid-Pliocene. These new data sets provide information on the geographic distribution of SST variability.

2. Materials and Methods

[6] The 77 records (Figure 2) used to create the PRISM2 SST reconstruction are the basic data used in this study. These represent marine cores and land sections from all the major ocean basins. Some localities represent time series,

¹U.S. Geological Survey, Reston, Virginia, USA.

²Goddard Institute for Space Studies, Columbia University, New York, New York, USA.

³Division of Earth and Ocean Sciences, Nicholas School of the Environment and Earth Sciences, Duke University, Durham, North Carolina, USA.

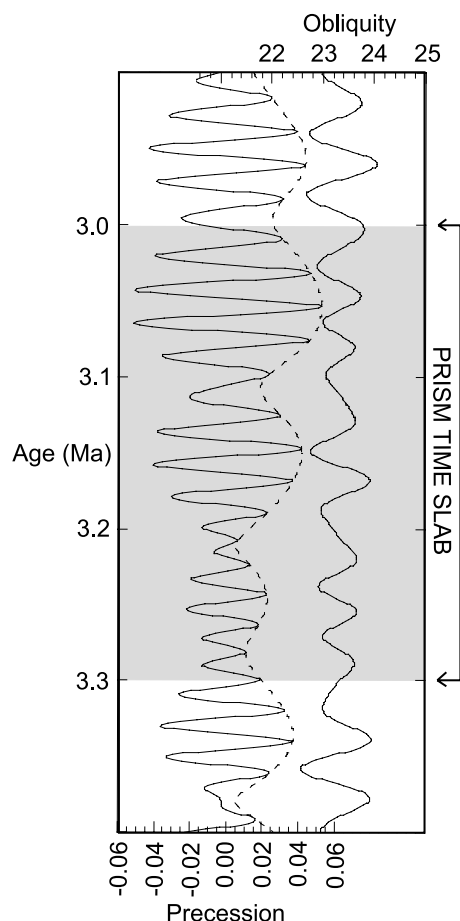


Figure 1. Orbital forcing within the Pliocene Research, Interpretation, and Synoptic Mapping (PRISM) time slab. Note low-amplitude obliquity cycles throughout the mid-Pliocene with precessional cycles that build in amplitude from the earlier to later part of the PRISM time slab. Eccentricity is shown by dashed line tracing upper limit of precession.

whereas others represent a handful of samples that can be correlated to the PRISM time slab. Data points are based primarily on planktic foraminifer assemblages, but also include ostracod, radiolaria and diatom data.

2.1. PRISM2 Reconstruction

[7] The PRISM2 reconstruction evolved from a series of studies that summarized conditions at a large number of marine and terrestrial sites and areas [e.g., Dowsett and Cronin, 1991; Poore and Sloan, 1996]. The first marine reconstruction was done by Dowsett and Poore [1991] for the North Atlantic and compared Pliocene SST to last interglacial conditions. That work concluded that although the North Atlantic was little different during the last interglacial than it is today, it was warmer during the mid-Pliocene. With added data, Dowsett *et al.* [1992] determined the Pliocene anomaly (Pliocene SST minus modern conditions) for the North Atlantic region and showed by means of a transect that middle- and high-latitude SST was warmer during the Pliocene than either the last interglacial or

present day. Conversely, low-latitude SST showed undetectable changes during climate extremes (Last Glacial Maximum, last interglacial, and mid-Pliocene). These results favored an increased meridional ocean heat transport over increased CO_2 as the forcing behind mid-Pliocene warming.

[8] Barron [1992], Ikeya and Cronin [1993], and Cronin *et al.* [1993] provided new data from the Pacific and circum-Arctic regions that was used to produce the first northern hemisphere SST reconstruction for the mid-Pliocene [Dowsett *et al.*, 1994]. One of the chief findings of that reconstruction was the documentation of warming in the Pacific at essentially the same time as the North Atlantic warming, suggesting that the mid-Pliocene warming was more than a regional event.

[9] By 1996, a number of southern hemisphere sites had been analyzed for foraminifers, diatoms and ostracods, and the first mid-Pliocene global reconstruction of SST was produced [Dowsett *et al.*, 1996]. That first global reconstruction of mid-Pliocene climate (PRISM1) was based upon 64 marine and 74 terrestrial sites and included data sets representing annual vegetation, land ice, monthly SST, sea ice, sea level and topography [Dowsett *et al.*, 1996; Thompson and Fleming, 1996].

[10] PRISM2 was a revision of PRISM1, incorporating additional marine sites to improve geographic coverage. For example, sites from the Mediterranean Sea and Indian Ocean were included for the first time. All SST estimates were recalculated using a new core top calibration based upon the Reynolds and Smith [1995] adjusted optimum interpolation (AOI) data set. The Pliocene sea level was reset at +25 m in keeping with reevaluation of isotopic and other data [Haq *et al.*, 1987; Dowsett and Cronin, 1990; Wardlaw and Quinn, 1991; Krantz, 1991; Wilson, 1993; Shackleton *et al.*, 1995]. PRISM2 used model results to guide the areal and topographic distribution of Antarctic ice, which resulted in a more realistic Antarctic ice configuration in tune with the 25 m sea level rise.

[11] The PRISM2 reconstruction consists of a series of 28 global-scale data sets on a 2° latitude by 2° longitude grid. For detailed information on these components and how they were created see Dowsett *et al.* [1999, and references therein].

2.2. Chronology

[12] The PRISM2 reconstruction is a global synthesis of a period of relatively warm and stable climate lying between the transition of marine oxygen isotope stages M2/M1 and G19/G18 [Shackleton *et al.*, 1995] in the middle part of the Gauss Normal Polarity Chron (C2An) (Figure 3). The reconstruction spans the interval of 3.29 Ma to 2.97 Ma (geomagnetic polarity timescales of Berggren *et al.* [1995], astronomically tuned timescale of Lourens *et al.* [1996]). It ranges from near the bottom of C2An1 (just above Kaena reversed polarity) to within C2An2r (Mammoth reversed polarity). This interval correlates to planktonic foraminiferal zones PL3 and PL4 or *Globorotalia margaritae-Sphaeroidinellopsis seminulina* and *Dentoglobigerina altispira-Globorotalia pseudomiocenica* planktic foraminiferal zones of Berggren [1973, 1977]. It falls within

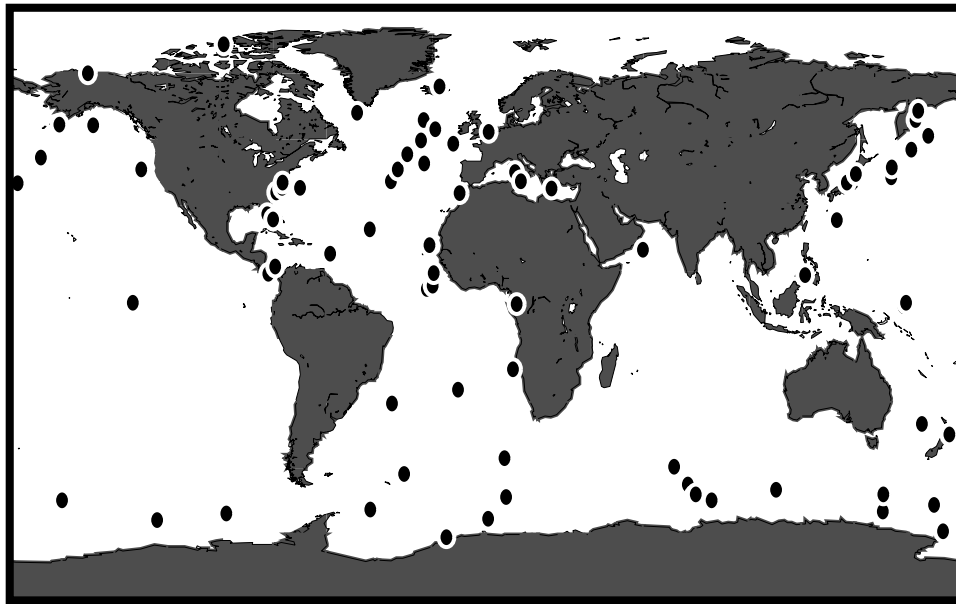


Figure 2. Geographic distribution of localities used to construct PRISM2 [Dowsett *et al.*, 1999], PRISM-MAX, and PRISM-MIN reconstructions.

calcareous nannofossil zone NN16 of Martini [1971] or CN12a of Bukry [1973, 1975].

2.3. Sea Surface Temperature Estimates and Peak Averaging

[13] Seventy-seven marine localities/sections were used for the PRISM2 SST reconstructions (Figure 2). The uneven distribution of control points used for the reconstruction primarily reflects the availability of suitable material for study. Details of the techniques used to transform fossil data into estimates of SST are given by Dowsett and Poore [1991], Dowsett [1991], Cronin and Dowsett [1990], Barron [1996], PRISM Project Members [1996], and Dowsett and Robinson [1998]. When available, estimates published by other workers were used to augment and cross check the estimates derived by the PRISM2 study.

[14] The peak averaging method [Dowsett and Poore, 1991] examines an SST time series for contained warm peaks. Those identified estimates that are considered valid are summed and averaged to provide a “warm peak average.” These average values, for each locality, are then contoured to produce SST reconstructions. By convention, the cold or winter SST string is examined for peaks and the corresponding warm or summer season estimates are also tabulated [Dowsett and Poore, 1991] (Figure 4).

[15] The “validity test” in most cases is a communality or distance measure cutoff. When using factor analytic transfer functions, the communality h^2 is given by the formula:

$$h_k^2 = \sum_{i=1}^k S_k^2$$

where the square of the correlation of variable k with factor i gives the part of the variance accounted for by that factor or the proportion of information explained by the chosen factor model. Therefore communality ranges from 0 to 1.

For example, a model that explains 80% of a multivariate sample's variance has a sample communality of 0.640. The PRISM reconstructions routinely use a communality threshold of 0.70 indicating the factor model explains a minimum of approximately 84% of the variance in the data.

[16] The modern analog technique, used heavily in the Pacific where modern calibration data have poor geographic

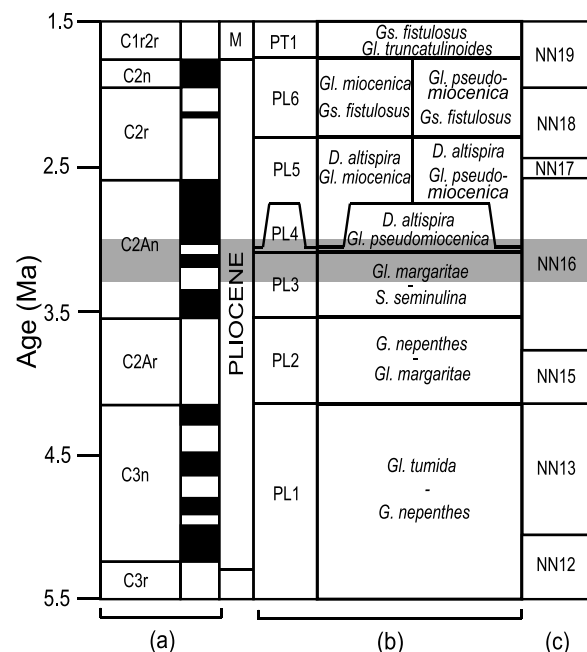


Figure 3. Correlation diagram showing position of (a) PRISM time slab interval (shaded band) relative to geomagnetic polarity, (b) planktic foraminiferal zones, and (c) calcareous nannofossil zonation [Berggren, 1973, 1977; Berggren *et al.*, 1995; Martini, 1971].

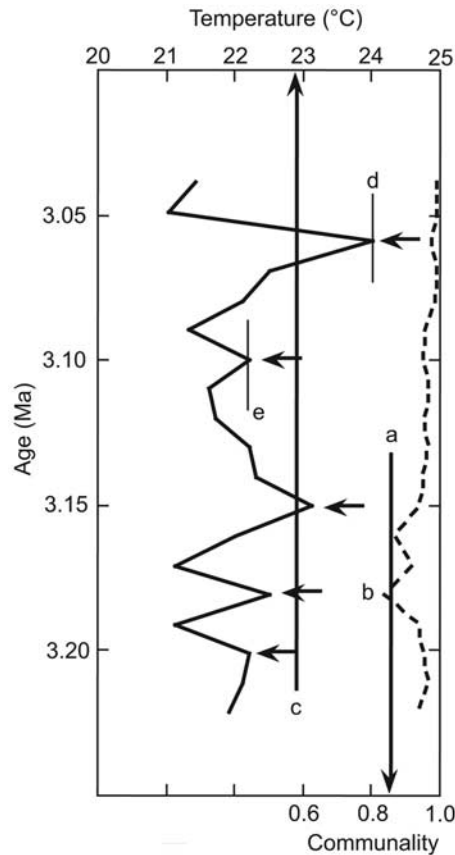


Figure 4. Hypothetical sea surface temperature (SST) record illustrating warm peak average (PRISM2), maximum warming (PRISM-MAX), and minimum warming (PRISM-MIN), as described in text. Solid jagged line represents SST estimates from factor analytic transfer function [Dowsett and Poore, 1990; Dowsett, 1991]. Dashed line shows down-core communality estimates. Vertical line (labeled a) pointing to the communality axis indicates communality of 0.85 (92% of variance explained by factor model). Horizontal arrows indicate warm peaks. Note that one warm peak (labeled b) near 3.175 Ma has a communality less than the chosen threshold of 0.85 and is therefore not used to develop the warm peak average ($\sim 22.8^{\circ}\text{C}$, indicated by vertical line (labeled c) pointing toward the SST axis) for the interval. Maximum warming (labeled d) and minimum warming (labeled e) as defined in text are also shown.

coverage, provides a distance measure between the target sample and the nearest analogs in a calibration data set. PRISM temperature estimates utilize the squared chord distance measure

$$d_{ij} = \sum k \left(p_{ik}^{1/2} - p_{jk}^{1/2} \right)^2$$

where d_{ij} is the squared chord distance between two multivariate samples i and j , and p_{ik} is the proportion of species k in sample i . Squared chord distance values can range from 0.0 to 2.0, with 0.0 indicating identical proportions of species within the samples being compared. Values above 0.15 are considered nonanalogs for the

purpose of our temperature estimation [Dowsett and Robinson, 1998; Dowsett and Poore, 1999]. We do not use the SIMMAX method of analogs [Pflaumann et al., 1996], despite improvements it offers, because of the geographic bias inherent in the methodology [Telford et al., 2004].

[17] In the example shown in Figure 4, the four warm peaks passing the validity test (in this case set to a communality = 0.85) have a mean value of 22.8°C . The PRISM methodology would use this value to represent how warm it gets during warm peak phases of the interval being investigated. The warmest peak on Figure 4 is $\sim 24.0^{\circ}\text{C}$ and the “coolest” warm peak still passing the validity test is just over 22°C . In this study, these maximum and minimum warm peaks within the PRISM time slab were recorded for each marine locality.

3. Results

[18] Each locality used in the PRISM2 reconstruction [Dowsett et al., 1999] was reevaluated in terms of chronology and accuracy of faunal census. For planktic foraminifer samples, transfer functions or dissimilarity coefficient matching was used to generate time series of SST for each site. Localities used for SST reconstruction range from detailed high-resolution time series from deep-sea cores to single samples from outcrop sections. The data primarily come from the former, but there are complications when determining the range of variability in some samples. Therefore, in sequences with too few samples or where other methods are not applicable, the error bars on the actual SST estimates were used to determine maximum and minimum probable warming.

[19] Following the methods outlined above, automated routines were applied to each time series to determine the warm peak average, maximum possible warming, and minimum possible warming. The warm peak averages were identical in all cases to the numbers generated by PRISM2. For both the maximum and minimum data, new anomaly maps were generated showing the difference between the warming scenario and the modern temperature at each site. These data were then used to construct contour maps of the maximum (minimum) warming anomalies relative to the PRISM2 reconstruction and modern temperature. These anomaly maps were applied to the PRISM2 temperature fields to generate new SST maps. As was the methodology for PRISM2, these transformations were done for February and August reconstructions, and the remaining 10 months of the year were generated by fitting each cell designated as marine to a sine curve. The final maximum (minimum) SST fields were then compared to PRISM2 sea ice maps. The maximum warming data set incorporates a simple 1-month shift in sea ice conditions resulting in a temporal increase in Northern Hemisphere ice-free conditions during summer. The minimum warming data set is not significantly different from the PRISM2 SST reconstruction to warrant changes in sea ice distribution, nor are there any independent data to support such changes.

4. PRISM-MAX Data

[20] The PRISM-MAX_{FEB,AUG} data are at first glance very similar to those of the PRISM2_{FEB,AUG} reconstruction

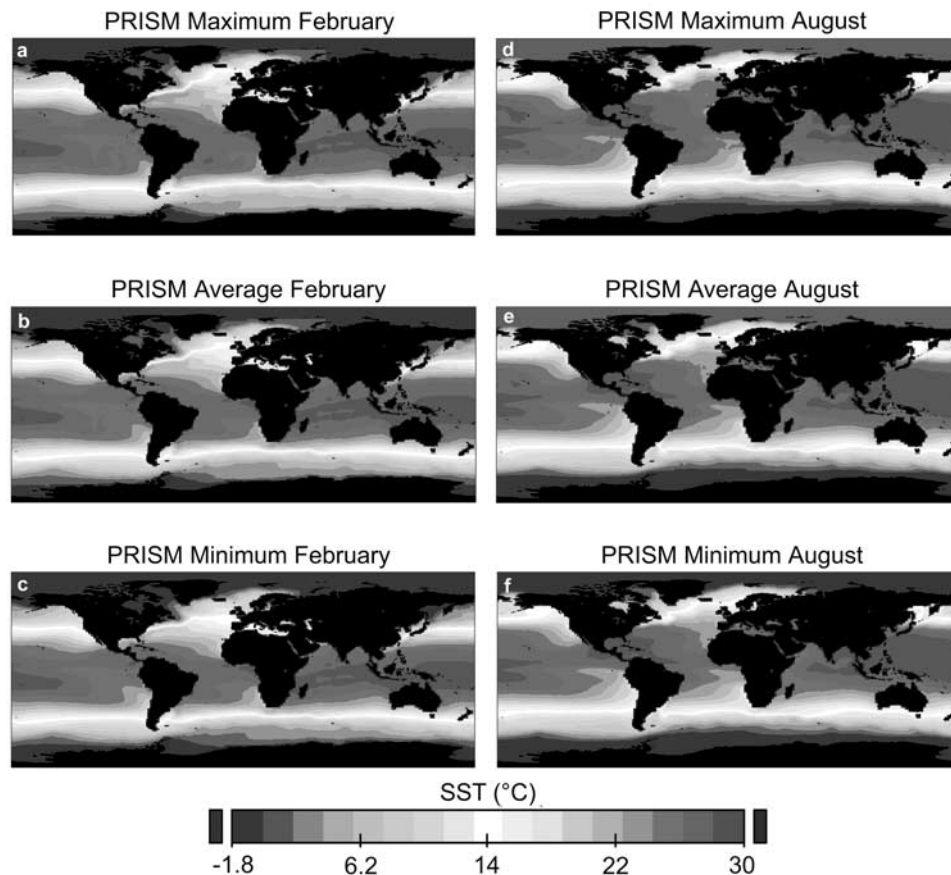


Figure 5. Maximum, minimum, and average (PRISM2) SST for February (a) PRISM-MAX, (b) PRISM2 and (c) PRISM-MIN and August (d) PRISM-MAX, (e) PRISM2, and (f) PRISM-MIN. See color version of this figure at back of this issue.

(Figure 5). On closer inspection, however, there are several significant differences. The movement of the 14°C isotherm illustrates the deflection of the warm waters of the Atlantic and Pacific Oceans toward the poles in both hemispheres. The effect of the Gulf Stream and Kuroshio Currents in the Northern Hemisphere are felt farther into the Arctic than during the average (PRISM2) reconstruction in both seasons. SST's along the Arctic shoreline are approximately 1.5 times warmer than those in the PRISM2 data set.

[21] Similar warming is found in the Southern Hemisphere where warmer waters in the PRISM-MAX reconstruction extend at least 2° latitude farther south than those within the PRISM2 reconstruction. The low-latitude regions show little to no warming with respect to modern SST in either the PRISM2 or the PRISM-MAX data.

[22] Sea ice distribution in the PRISM-MAX_{FEB,AUG} reconstruction shows approximately 5% less annual sea ice cover than in the PRISM2 reconstruction. The seasonal distribution of sea ice in both hemispheres shows a longer period of summer ice-free conditions, and a maximum extent of winter sea ice that is somewhat less than in the PRISM2 reconstruction. SST data along sea ice margins was adjusted to make a

smooth transition between the sea ice and open marine regions.

5. PRISM-MIN Data

[23] The PRISM-MIN_{FEB,AUG} data are similar to those of the PRISM2 reconstruction. The 14° isotherm can again be used to discern subtle differences between this and the PRISM2 reconstruction. As one might expect, SST's are deflected toward the equator to a small degree just as the SST's in PRISM-MAX were deflected toward the polar regions. The reduction in warming is less significant and represents on average approximately 75% of the PRISM2 warming outside of low-latitude regions in both hemispheres. With SST's so similar to the PRISM2 reconstruction, sea ice in PRISM-MIN was left unchanged from the PRISM2 configuration.

6. Discussion

6.1. Variability of Warming Within the PRISM Time Slab

[24] The PRISM-MAX and PRISM-MIN analyses indicate that variability of warming in the low latitudes was small compared to middle- and high-latitude areas. The greatest

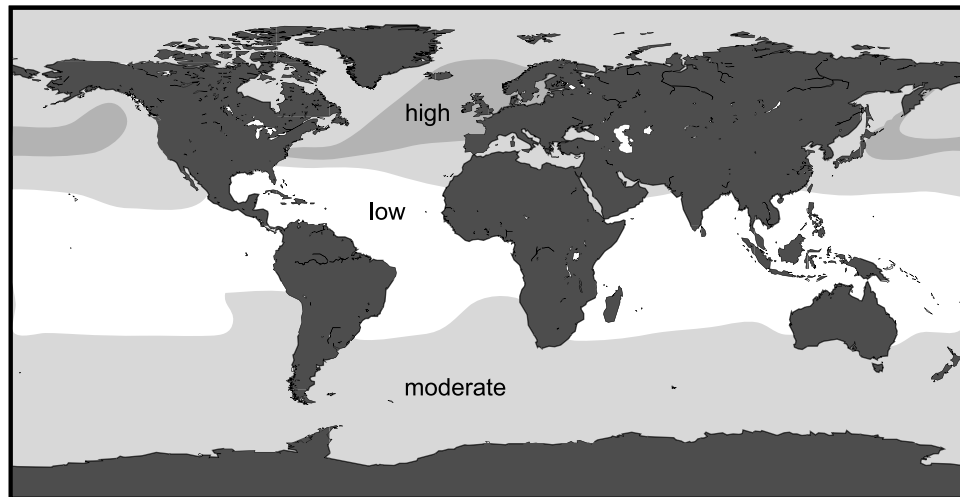


Figure 6. Variability of Pliocene derived by subtracting PRISM-MIN from PRISM-MAX, based upon the 77 PRISM localities shown in Figure 2.

variability is seen in regions that experienced the greatest warming (Figure 6). On a broad scale, these areas of increased variability probably reflect variations in the positions of the warm poleward flowing currents of the main gyres. In these areas, rapid or abrupt climate changes within the PRISM time slab occur over periods of less than 5000 years. *Draut et al.* [2003] document variability in the oxygen isotopic record of surface dwelling planktics that exhibits transitions of up to 0.6‰ in only 4000 years. Over this same interval, preliminary work on planktic foraminiferal assemblages indicates a $\sim 2^{\circ}\text{C}$ change in SST. The abruptness of these changes is controlled by stratigraphic resolution (and therefore sample density), and is probably much shorter, although additional work is necessary to refine these data.

[25] It is important to note that the warming variability referred to here is not a measure of the range of SST within the time slab but rather the range in the “estimated warming” within the time slab. Overall range in temperature is usually significantly greater than the values reported here.

6.2. Geographic Distribution of Warming Relative to Modern Conditions

[26] PRISM results using planktic foraminiferal SST estimates have documented low-latitude temperatures that exhibit little discernible change from present-day conditions. The pattern of greater warming with increasing latitude reconstructed by the PRISM analyses has been used to support the hypothesis that increased meridional ocean heat flux contributed to Pliocene warmth [Dowsett et al., 1992]. Increasing poleward ocean heat transport would even have the effect of cooling at the equator [Rind and Chandler, 1991]. Another hypothesis to account for Pliocene climate warmth in middle to high latitudes is increased atmospheric CO_2 , which would have the effect of constant magnitude of warming at all latitudes, amplified where sea ice is removed. In fact, a combination of the two mechanisms was probably responsible for the Pliocene record of warmth [Sloan et al., 1995; Raymo et al., 1996].

[27] Recent work on Pliocene SST results from alkenone paleothermometry indicates warming may have also occurred in some low-latitude regions, in contrast to the planktic foraminifer faunal based SST estimates presented previously and expanded upon in the current paper.

[28] From an ecological standpoint, it seems unlikely that open ocean tropical SST during the Pliocene rose above $30^{\circ}\text{--}31^{\circ}\text{C}$. Laboratory culture studies indicate that $\sim 31^{\circ}\text{C}$ is an upper limit of planktic foraminifer survival [Bijma et al., 1990]. If Pliocene temperatures were significantly warmer than today, one would expect a Pliocene tropical foraminiferal assemblage composition distinct from those of the modern tropics. For example, there might be higher percentages of the most thermophilic species *Globigerinoides ruber* and *Globigerinoides sacculifer*. Indeed, surface temperatures in the modern Red Sea reach values in excess of 32°C [Reynolds and Smith, 1995] and contain low-diversity planktic foraminifer assemblages dominated by *Globigerinoides ruber* and *Globigerinoides sacculifer* [Kroon, 1991]. Our mid-Pliocene low-latitude planktic assemblages do not have the same structure. A less likely alternative is that modern tropical foraminiferal assemblages maintained their modern community structure even in response to temperatures above $\sim 30^{\circ}\text{C}$.

[29] A compilation of mid-Pliocene alkenone-based SST estimates [Haywood et al., 2005] contains five localities, primarily from areas of ocean margin or equatorial upwelling [Herbert and Schuffert, 1998; Marlow et al., 2000]. Changes in upwelling regions are not necessarily indicative of overall low-latitude warming, but may instead be a local to regional phenomenon. Thus alkenone spatial coverage is still limited compared to the PRISM2 foraminiferal locality distribution. Moreover, few alkenone sites are near PRISM2 locations, making direct comparison of the two proxy methods difficult.

[30] A carefully planned program using multiproxy temperature estimation on the same sample sets from both upwelling and nonupwelling regions and a range of latitudes is necessary to adequately address the question of Pliocene

low-latitude temperatures. Such a study will also need to address interproxy calibration differences [Muller *et al.*, 1998; Dowsett *et al.*, 1999] (presently the alkenone calibration shows on average 0.5°C ranging up to 2°C warmer temperatures than the PRISM calibration) and interspecific and intraspecific variability of alkenone values [Conte *et al.*, 1998] in light of the differences in the calcareous nannofossil floras between modern and Pliocene sediments.

7. Conclusions

[31] Modeling experiments utilizing the PRISM reconstructions [i.e., Chandler *et al.*, 1994; Sloan *et al.*, 1996; Haywood *et al.*, 2000; Haywood *et al.*, 2001; Haywood and Valdes, 2004] have shown that results are heavily influenced by the ocean conditions set in the model. It is not clear whether coupled ocean-atmosphere modeling experiments [e.g., Haywood and Valdes, 2004] can accurately portray the mid-Pliocene climate without a better understanding of deep ocean conditions [Cronin *et al.*, 2005], low-latitude SST, and some idea of the variability of mid-Pliocene warming. Together with the modeling community, PRISM researchers have devised the maximum and minimum possible warming data sets presented here as a bracket around oceanic climatic conditions during the mid-Pliocene.

[32] Clearly, the peak averaging method produces a reconstruction that is flawed. The inability to correlate

accurately between submillennial to millennia scale events occurring more than 3 million years ago is the chief reason for this. The PRISM-MAX and PRISM-MIN data sets developed here are likewise unrealistic, but they place an outside bound on the state of the climate system during the mid-Pliocene warm period. Together, they define the variability of warming within the PRISM time slab. These new minimum and maximum possible warming data are particularly useful for climate modeling studies where it is necessary to calculate the range of SST forcing within the PRISM time slab.

[33] The results presented here indicate greatest variability in warming within the PRISM time slab occurs in middle- to high-latitude regions where the greatest warming relative to present has previously been documented. Comparison of multiproxy records (faunal, alkenone and Mg:Ca) from individual locations within and away from upwelling regions are necessary to address the important question of low-latitude warming (relative to present) during the mid-Pliocene.

[34] **Acknowledgments.** This work benefited from discussions with Alan Haywood and Debra Willard. Lynn Wingard, Marci Robinson, and Mark Williams provided helpful reviews of this manuscript. Funding for this work was provided by the USGS Earth Surface Dynamics Program (H.J.D. and T.M.C.) and the National Science Foundation (ATM-0214400 and ATM-0323516 to M.A.C. and ATM-0323276 to G.S.D.).

References

- Barron, J. A. (1992), Pliocene paleoclimatic interpretation of DSDP Site 580 (NW Pacific) using diatoms, *Mar. Micropaleontol.*, 20, 23–44.
- Barron, J. A. (1996), Diatom constraints on the position of the Antarctic Polar Front in the middle part of the Pliocene, *Mar. Micropaleontol.*, 27, 195–213.
- Berggren, W. A. (1973), The Pliocene time scale: Calibration of planktonic foraminiferal and calcareous nannoplankton zones, *Nature*, 243, 391–397.
- Berggren, W. A. (1977), Late Neogene planktonic foraminiferal biostratigraphy of the Rio Grande Rise (South Atlantic), *Mar. Micropaleontol.*, 2, 265–313.
- Berggren, W. A., D. V. Kent, C. C. Swisher, and M.-P. Aubry (1995), A revised Cenozoic geochronology and chronostratigraphy, in *Geochronology, Time Scales and Global Stratigraphic Correlation*, edited by W. A. Berggren *et al.*, Tulsa, *Spec. Publ. SEPM Soc. Sediment. Geol.*, 54, 129–212.
- Bijma, J., W. W. Faber, and C. Hemleben (1990), Temperature and salinity limits for growth and survival of some planktonic foraminifers in laboratory cultures, *J. Foraminiferal Res.*, 20(2), 95–116.
- Bukry, D. (1973), Low-latitude coccolith biostratigraphic zonation, *Initial Rep. Deep Sea Drill. Project*, 15, 685–703.
- Bukry, D. (1975), Coccolith and silicoflagellate stratigraphy, northwestern Pacific Ocean, Deep Sea Drilling Project Leg 32, *Initial Rep. Deep Sea Drill. Proj.*, 32, 677–701.
- Chandler, M., D. Rind, and R. Thompson (1994), Joint investigations of the middle Pliocene climate II: GISS GCM Northern Hemisphere results, *Global Planet. Change*, 9, 197–219.
- Conte, M. H., A. Thompson, D. Lesley, and R. S. Harris (1998), Genetic and physiological influences on the alkenone/alkenone versus growth temperature relationship in *Emiliania huxleyi* and *Gephyrocapsa oceanica*, *Geochim. Cosmochim. Acta*, 62, 51–68.
- Cronin, T. M., and H. J. Dowsett (1990), A quantitative micropaleontologic method for shallow marine paleoclimatology: Application to Pliocene deposits of the western North Atlantic Ocean, *Mar. Micropaleontol.*, 16, 117–148.
- Cronin, T. M., R. C. Whitley, A. Wood, A. Tsukagoshi, N. Ikeya, E. Brouwers, and W. Briggs (1993), Microfaunal evidence for elevated Pliocene temperatures in the Arctic Ocean, *Paleoceanography*, 8(2), 161–173.
- Cronin, T. M., H. J. Dowsett, G. S. Dwyer, P. A. Baker, and M. A. Chandler (2005), Mid-Pliocene deep-sea bottom water temperatures based on ostracode Mg/Ca ratios, *Mar. Micropaleontol.*, 54, 249–261.
- Dowsett, H. J. (1991), The development of a long-range foraminifer transfer function and application to late Pleistocene North Atlantic climatic extremes, *Paleoceanography*, 6(2), 259–273.
- Dowsett, H. J. (2004), Bracketing mid Pliocene sea surface temperature: Maximum and minimum possible warming, *U.S. Geol. Surv. Data Ser.*, 114. (Available at <http://pubs.usgs.gov/ds/2004/114/>)
- Dowsett, H. J., and T. M. Cronin (1990), High eustatic sea level during the Middle Pliocene: Evidence from the southeastern U.S. Atlantic Coastal Plain, *Geology*, 18, 435–438.
- Dowsett, H. J., and T. M. Cronin (1991), Preface, *Quat. Sci. Rev.*, 10(2–3), v–vi.
- Dowsett, H. J., and R. Z. Poore (1991), Pliocene sea surface temperatures of the North Atlantic Ocean at 3.0 Ma, *Quat. Sci. Rev.*, 10(2–3), 189–204.
- Dowsett, H. J., and R. Z. Poore (1999), Last interglacial sea surface temperature estimates from the California margin: Improvements to the modern analog technique, *U.S. Geol. Surv. Bull.*, 2171. (Available at <http://pubs.usgs.gov/bulletin/b2171/>)
- Dowsett, H. J., and M. M. Robinson (1998), Application of the modern analog technique (MAT) of sea surface temperature estimation to middle Pliocene North Pacific planktonic foraminifer assemblages, *Palaeontol. Electron.*, 1(1), article 3, 22 pp. (Available at http://palaeo-electronica.org/1998_1/dowsett/issue1.htm)
- Dowsett, H. J., T. M. Cronin, R. Z. Poore, R. C. Whitley, and A. Wood (1992), Evidence for increased meridional heat transport in the North Atlantic Ocean during the Pliocene, *Science*, 258, 1133–1135.
- Dowsett, H. J., R. S. Thompson, J. A. Barron, T. M. Cronin, R. F. Fleming, S. E. Ishman, R. Z. Poore, D. A. Willard, and T. R. Holtz Jr. (1994), Paleoclimatic reconstruction of a warmer Earth: PRISM middle Pliocene Northern Hemisphere synthesis, *Global Planet. Change*, 9, 169–195.
- Dowsett, H. J., J. A. Barron, and R. Poore (1996), Middle Pliocene sea surface temperatures: A global reconstruction, *Mar. Micropaleontol.*, 27(1–4), 13–25.
- Dowsett, H. J., J. A. Barron, R. Z. Poore, R. S. Thompson, T. M. Cronin, S. E. Ishman, and

- D. A. Willard (1999), Pliocene paleoenvironmental reconstruction: PRISM2, *U.S. Geol. Surv. Open File Rep.*, 99–535. (Available at <http://pubs.usgs.gov/of/of99-535/>)
- Draut, A. E., M. E. Raymo, J. F. McManus, and D. W. Oppo (2003), Climate stability during the Pliocene warm period, *Paleoceanography*, 18(4), 1078, doi:10.1029/2003PA000889.
- Haq, B. H., J. Hardenbol, and P. R. Vail (1987), Chronology of fluctuating sea levels since the Triassic, *Science*, 235, 1156–1167.
- Haywood, A. M., and P. J. Valdes (2004), Modelling Pliocene warmth: Contribution of atmosphere, oceans and cryosphere, *Earth Planet. Sci. Lett.*, 218, 363–377.
- Haywood, A. M., P. J. Valdes, and B. W. Sellwood (2000), Global scale palaeoclimate reconstruction of the middle Pliocene climate using the UKMO GCM: Initial results, *Global Planet. Change*, 25, 239–256.
- Haywood, A. M., P. J. Valdes, B. W. Sellwood, J. O. Kaplan, and H. J. Dowsett (2001), Modelling middle Pliocene warm climates of the USA, *Palaeontol. Electron.*, 4(1), article 5, 21 pp. (Available at http://palaeo-electronica.org/2001_1/climate/issue1_01.htm)
- Haywood, A. M., P. Dekens, A. C. Ravelo, and M. Williams (2005), Warmer tropics during the mid-Pliocene? Evidence from alkenone paleothermometry and a fully coupled ocean-atmosphere GCM, *Geochim. Geophys. Geosyst.*, 6, Q03010, doi:10.1029/2004GC000799.
- Herbert, T. D., and J. D. Schuffert (1998), Alkenone unsaturation estimates of late Miocene through late Pliocene sea surface temperature changes, ODP Site 958, *Proc. Ocean Drill. Program Sci. Results*, 159, 17–22.
- Ikeya, N., and T. M. Cronin (1993), Quantitative analysis of ostracoda and water masses around Japan: Application to Pliocene and Pleistocene paleoceanography, *Micropaleontology*, 39, 263–281.
- Krantz, D. E. (1991), A chronology of Pliocene sea-level fluctuations: The U.S. middle Atlantic Coastal Plain record, *Quat. Sci. Rev.*, 10(2–3), 163–174.
- Kroon, D. (1991), Distribution of extant planktic foraminiferal assemblages in Red Sea and northern Indian Ocean surface waters, *Rev. Espan. Micropaleontol.*, 23(1), 37–74.
- Lourens, L. J., A. Antonarakou, F. J. Hilgen, A. A. M. Van Hoof, C. Vergnaud-Grazzini, and W. J. Zachariasse (1996), Evaluation of the Plio-Pleistocene astronomical timescale, *Paleoceanography*, 11(4), 391–413.
- Marlow, J. R., C. B. Lange, G. Wefer, and A. Rosell-Mele (2000), Upwelling intensification as part of the Plio-Pleistocene climate transition, *Science*, 290, 2288–2294.
- Martini, E. (1971), Standard tertiary and Quaternary calcareous nannoplankton zonation, in *Proceedings II Planktonic Conference, Rome, 1970*, vol. 2, edited by A. Farinacci, pp. 739–785, Telao Sci., Rome.
- Muller, P. J., G. Krist, G. Ruhland, I. Von Storch, and A. Rosell-Mele (1998), Calibration of the alkenone paleotemperature index UK'₃₇ based on core-tops from the eastern South Atlantic and the global ocean (60N–60S), *Geochim. Cosmochim. Acta*, 62, 1757–1772.
- Pflaumann, U., J. Duprat, C. Pujol, and L. Labeyrie (1996), SIMMAX: A modern analog technique to deduce Atlantic sea surface temperatures from planktic foraminifera in deep sea sediments, *Paleoceanography*, 11(1), 15–35.
- Poore, R. Z., and L. C. Sloan (1996), Climates and climate variability of the Pliocene, *Mar. Micropaleontol.*, 27(1/4), 1–2.
- PRISM Project Members (1996), Middle Pliocene paleoenvironments of the Northern Hemisphere, *Paleoclimate and Evolution, With Emphasis on Human Origins*, edited by E. S. Vrba et al., pp. 197–212, Yale Univ. Press, New Haven, Conn.
- Raymo, M. E., B. Grant, M. Horowitz, and G. H. Rau (1996), Mid-Pliocene warmth: Stronger greenhouse and stronger conveyor, *Mar. Micropaleontol.*, 27(1/4), 313–326.
- Reynolds, R. W., and T. M. Smith (1995), A high-resolution global sea surface temperature climatology, *J. Clim.*, 8, 1571–1583.
- Rind, D., and M. A. Chandler (1991), Increased ocean heat transports and warmer climate, *J. Geophys. Res.*, 96, 7437–7461.
- Shackleton, N. J., M. A. Hall, and D. Pate (1995), Pliocene stable isotope stratigraphy of Site 846, *Proc. Ocean Drill. Program Sci. Results*, 138, 337–355.
- Sloan, L. C., J. C. G. Walker, and T. C. Moore Jr. (1995), Possible role of oceanic heat transport in early Eocene climate, *Paleoceanography*, 10(2), 347–356.
- Sloan, L. C., T. J. Crowley, and D. Pollard (1996), Modeling of middle Pliocene climate with the NCAR GENESIS general circulation model, *Mar. Micropaleontol.*, 27, 51–61.
- Telford, R. J., C. Andersson, H. J. B. Birks, and S. Juggins (2004), Biases in the estimation of transfer function prediction errors, *Paleoceanography*, 19, PA4014, doi:10.1029/2004PA001072.
- Thompson, R. S., and R. F. Fleming (1996), Middle Pliocene vegetation: Reconstructions, paleoclimatic inferences, and boundary conditions for climate modeling, *Mar. Micropaleontol.*, 27(1/4), 27–49.
- Wardlaw, B. R., and T. M. Quinn (1991), The record of Pliocene sea-level change at Enewetak Atoll, *Quat. Sci. Rev.*, 10(2/3), 247–258.
- Wilson, G. S. (1993), Ice induced sea level change in the late Neogene, Ph. D. thesis, Victoria Univ., Wellington.
- Zubakov, V. A., and I. I. Borzenkova (1988), Pliocene palaeoclimates: Past climates as possible analogues of mid-twenty-first century climate, *Palaeogeogr. Palaeoclimatol. Palaeoecol.*, 65, 35–49.
- Zubakov, V. A., and I. I. Borzenkova (1990), *Global Paleoclimate of the Late Cenozoic: Dev. Paleontol. Stratigr.*, vol. 12, 456 pp., Elsevier, New York.

M. A. Chandler, Goddard Institute for Space Studies, Columbia University, 2880 Broadway, New York, NY 10025, USA.

T. M. Cronin and H. J. Dowsett, U.S. Geological Survey, 926A National Center, Reston, VA 20192, USA. (hdowsett@usgs.gov)

G. S. Dwyer, Division of Earth and Ocean Sciences, Nicholas School of the Environment and Earth Sciences, Duke University, Durham, NC 27708, USA.

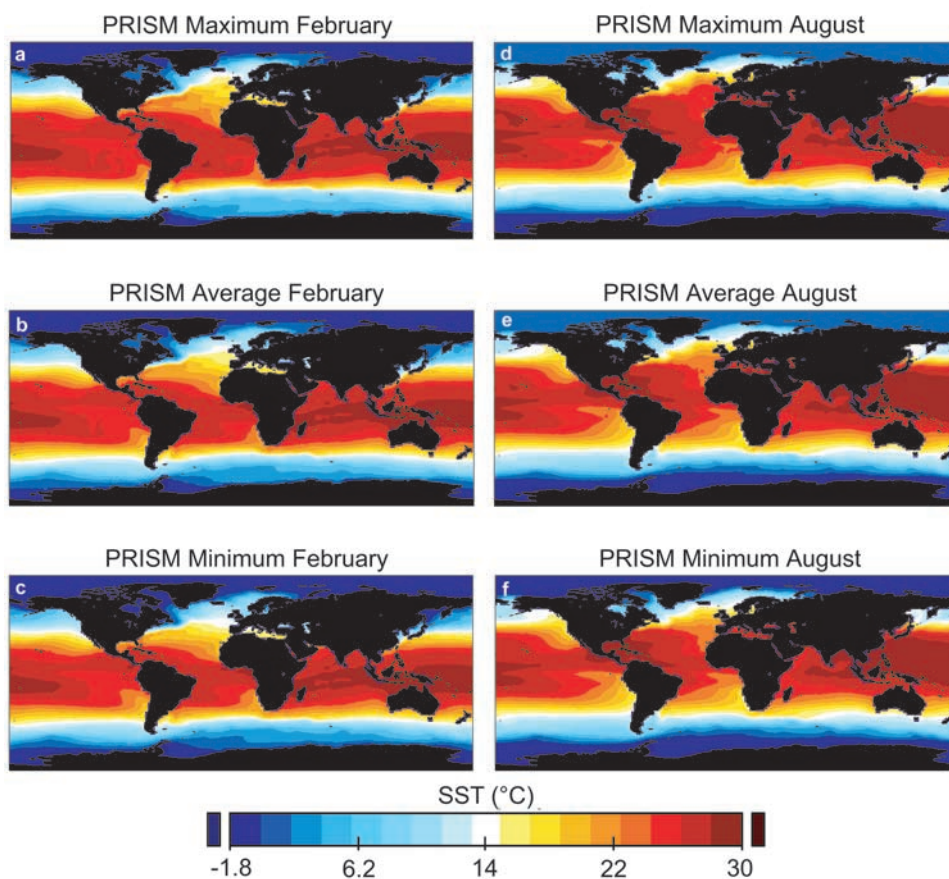


Figure 5. Maximum, minimum, and average (PRISM2) SST for February (a) PRISM-MAX, (b) PRISM2 and (c) PRISM-MIN and August (d) PRISM-MAX, (e) PRISM2, and (f) PRISM-MIN.